THE JOURNAL OF PHYSICAL CHEMISTRY C

Review Article

Cite This: J. Phys. Chem. C 2019, 123, 12029−12041

pubs.acs.org/JPCC

New Perspective of Mitigating the Coffee-Ring Effect: Interfacial Assembly

Karam Nashwan Al-Milaji and Hong Zhao*

Department of Mechanical and Nuclear Engineering, BioTech One, Virginia Commonwealth University, 800 East Leigh Street, Richmond, Virginia 23219, United States

ABSTRACT: The evaporation of particle-laden droplets on a substrate usually results in ring-like deposits due to particle migration to the contact lines. This ubiquitous phenomenon, known as the coffee-ring effect (CRE), was initially observed in drying coffee droplets and later in many colloidal systems. The CRE has been intensively investigated during the past two decades to unveil the complexity related to its flow patterns, evaporation physics, and deposition structures after solvent evaporation. However, the contribution of colloidal particle assembly and interactions at the air−liquid interface of sessile droplets to the particle deposition requires more attention. The objective of this Review Article is to highlight the recent advances in mitigating or totally suppressing the CRE by means of interfacial assembly via manipulating the multibody interactions, for example, particle−particle, particle−substrate, particle−flow, and particle−interface interactions. Well-ordered monolayer deposition of the colloidal particles, driven by interfacial assembly, has been demonstrated by several research groups. This unique perspective of suppressing the CRE and creating well-ordered monolayer structures by assembling colloidal particles at the air−liquid interface creates a new paradigm in generating coatings and functional devices through liquid processing. General rules and guidelines are established to provide broader prospects of engineering desirable structures of colloidal particle deposition and assembly.

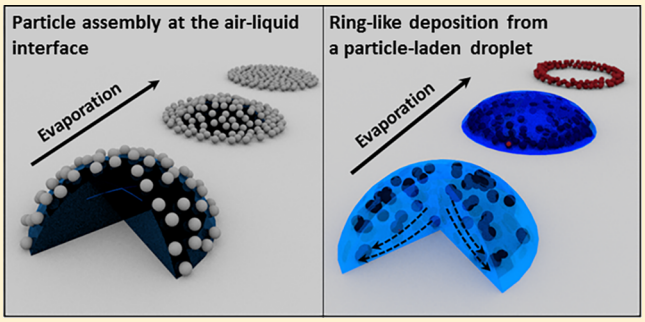

1. INTRODUCTION

Drying of particle-laden droplets on a substrate usually leaves ring-like deposits, which is known as the coffee-ring effect (CRE).[1−3] This ubiquitous phenomenon is familiar to everyone who has observed the drying of coffee spills. Deegan et al. were the pioneers who first investigated this remarkable observation two decades ago.[4−6] The driving force behind such an omnipresent process is the nonuniform evaporation flux taking place at the air−liquid interface of the sessile droplet, where it is found to be higher in vicinity of the three-phase contact line.[4,7] The greater liquid loss at the edges must be replenished from the bulk liquid of the sessile droplet. This, in turn, initiates an outward flow referred to as evaporation-induced flow, which drives the particles to the contact line.[4,8] As a result, a ring-like shape pattern is evolved as the solvent completely evaporates.

Following the seminal work of Deegan and coworkers, particle deposition and assembly structure obtained from evaporating particle-laden droplets have been a subject of a plethora of theoretical and experimental studies for scientific and industrial applications. The research endeavors to understand the drying of colloidal droplets revealed some crucial factors affecting the coffee-ring formation, in particular, surface wettability and contact line dynamics, solvent evaporation, and the properties of the colloidal particles (e.g., particle size and shape, functional groups, hydrophobicity, charge density of the particles, etc.).[9] To date, considerable efforts have been devoted to counteract the colloidal particle migration to the contact lines by means of controlling the drying conditions of solvents (e.g., substrate temperature,[10] relative humidity,[11] and volatile solvents[12]), modifying particle shapes,[13,14] changing solvent density and viscosity,[15] adjusting substrate wettability,[16,17] initiating acoustic field,[18] and exerting electrowetting.[19] Because the direct driving force of the CRE formation is the evaporation-induced flow, it is intuitive to change the deposition morphology by manipulating the flow pattern (e.g., generating a Marangoni flow) to guide the particles back to the center of the sessile droplet.[20−23] Please refer to the recent review papers on these aspects.[1,2,24] Therefore, understanding these different mechanisms is of significant importance for controlling the particle depositions, which is proven to be advantageous in a wide range of technological applications such as inkjet printing of electronic,[25−30] optical,[31,32] and biomedical devices,[33−35] to name a few. Although the CRE has been demonstrated as a potential tool to be implemented in many disciplines such as particle separation[36−38] and disease detection,[39,40] this phenomenon is deemed detrimental and must be avoided in many technological applications such as producing coatings and patterns,[41−43] fabricating functional microarrays,[44−46] and detecting biomolecules by various spectroscopy techniques.[47,48]

Received: January 26, 2019
Revised: April 6, 2019
Published: April 18, 2019

DOI: 10.1021/acs.jpcc.9b00797
J. Phys. Chem. C 2019, 123, 12029−12041

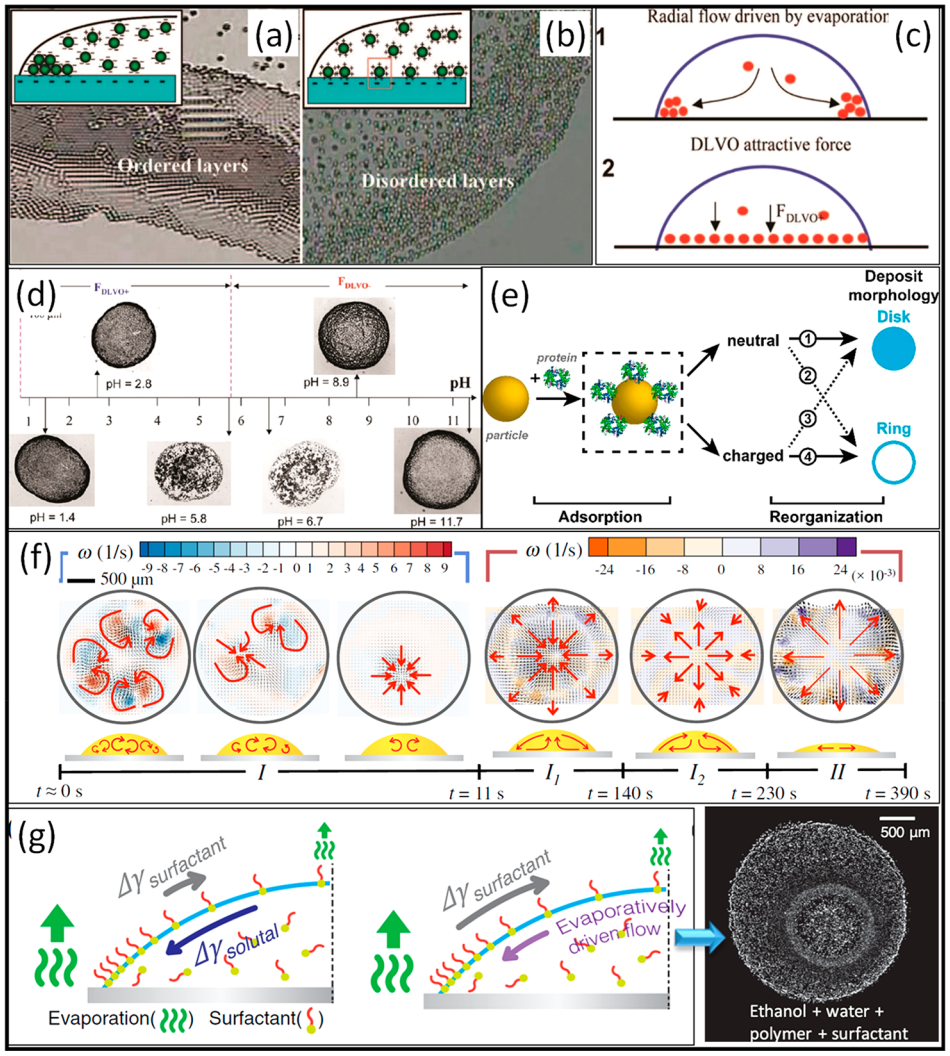

Figure 1. Assembly of (a) negatively charged colloidal particles and (b) positively charged colloidal particles at the edge of the sessile droplet on a negatively charged glass substrate, which demonstrates the order-to-disorder assembly structures at the contact line. Reprinted from ref 50. Copyright 2008 American Chemical Society. (c) Schematic illustration of the impact of DLVO force on the particle deposition, where a system lacking the DLVO interaction results in a ring formation, whereas having such attractive DLVO force renders more uniform particle depositions. (d) Particle deposition change with respect to pH value. Reprinted with permission from ref 51. Copyright 2010 American Chemical Society. (e) Illustration of the influence of protein adsorption on the particle deposition. Manipulating the surface charge of the colloidal particles resulted in different particle−particle and particle−substrate electrostatic and hydrophobic interactions, as indicated by the four routes. Reprinted with permission from ref 52. Copyright 2016 American Chemical Society. (f) Flow-field pattern representations observed in a drying whisky droplet and (g) schematics of solutal and surfactant Marangoni flows. The ethanol/water and surfactant mixtures do not produce uniform particle deposition unless they are combined with a polymer to enhance the particle adhesion to the substrate. Reprinted with permission from ref 54. Copyright 2016 American Physical Society.

Despite an excessive number of studies dedicated to this field, the mechanism behind the particle deposition and morphology of colloidal suspensions has not been fully understood yet,[49] especially for particles assembled at the air−liquid interface. This Review Article highlights the recent advances in mitigating or totally suppressing the CRE, even producing monolayer deposition of colloidal particles, through particle interfacial assembly. The first objective of this Review Article is to underline the significant importance of manipulating the multibody interactions (e.g., particle−particle, particle−substrate, and particle−interface interactions) in colloidal droplets to control the particle deposition and morphology. The second objective of this review is to present an alternative concept to mitigate or suppress the CRE through assembling the colloidal particles at the air−liquid interface of sessile droplets. This approach has been recently demonstrated as an effective tool for producing nearly monolayer, closely packed networks of self-assembled nanoparticles. The recent efforts in the simulation of particles at the air−liquid interface of an evaporating sessile droplet have been included as well.

2. MULTIBODY INTERACTIONS IN AN EVAPORATING PARTICLE-LADEN DROPLET

In an evaporating particle-laden droplet on a solid substrate, multiple bodies (e.g., colloidal particles with various functional groups and charge levels, solvent(s), substrates with different surface chemistry and heterogeneities, and ambient gas phase) interact with each other during solvent evaporation. Such intricate interactions affect droplet wetting and contact line pinning behavior (solvent−substrate interaction), evaporation-induced flow (air−liquid interaction), and ultimately particle deposition that is influenced by particle−particle, particle−flow,

DOI: 10.1021/acs.jpcc.9b00797
J. Phys. Chem. C 2019, 123, 12029−12041

particle−substrate, and particle−interface interactions. It is beneficial to introduce how the multibody interactions affect and direct the particle assembly and deposition because similar interactions could be utilized to enable particle assembly at the air−liquid interface.

Yan et al. studied the assembly of charged colloidal particles on charged glass substrates near the contact line of an evaporating sessile droplet.[50] The colloidal particle mobility and ordering in the vicinity of the contact line were highly impacted by the particle−substrate interactions. For colloidal particles possessing the same surface charge as the substrate, they were readily transported to the edge of the sessile droplet by virtue of the convective flow, resulting in ordered, self-assembled ring-like depositions. Conversely, opposite charges of colloidal particles and substrates led to a decrease in particle mobility and poor particle packing at the contact line region. The lack of particle orderliness was attributed to the strong Coulombic attraction forces between the spherical particles and the substrate, whereas no such Coulombic adhesion was present in systems with alike surface charges of particles and substrates (Figure 1a,b). Similar particle−substrate interactions were observed when ionic and nonionic surfactants were introduced to the system, affecting the final particle deposition. The authors also commented on the role of hydrophobic interactions between surfactant-coated particles and substrate, causing the particles to strongly adhere to the substrate.

Bhardwaj et al. examined the particle deposition obtained from drying nanoliter droplets containing titania nanoparticles on glass substrates.[51] Changing the pH of the suspension resulted in different particle depositions ranging from ring-like to uniform deposition structures. This transition in deposit patterns was explained by the Derjaguin−Landau−Verwey−Overbeek (DLVO) interactions (i.e., electrostatic and van der Waals forces) between the particles and the substrate. The zeta potential of the particles changed from positive to negative when the pH level of the suspension increased from low (acidic) to high (basic) conditions, whereas the glass substrate retained negative zeta potentials for most of the pH conditions. The deposition of titania nanoparticles at different pH values is presented in Figure 1c,d. In an extreme acidic environment, the particle deposition had a thin uniform film of particles with a thick ring of particles at the three-phase contact line. The particles close to the substrate were attracted toward the substrate under the attractive DLVO force as a result of the particle−substrate interaction, forming a uniform thin layer of nanoparticles. However, because the Debye length was much less than the droplet height, the rest of the suspended particles were carried by the capillary flow to the contact line, resulting in a thicker ring at the periphery. The titania nanoparticles were noticed to agglomerate and randomly scatter throughout the deposits at intermediate pH values. At this point, the titania nanoparticles became nearly neutral, leading to a weaker particle−substrate DLVO interaction than the van der Waals forces among the particles. Extremely basic environments, on the contrary, enhanced the repulsive particle−particle and particle−substrate DLVO interactions, preventing the nanoparticles from depositing onto the substrate. As a result, most of the particles followed the outward radial flow and accumulated at the contact line.

Devineau et al. investigated how the adsorption of charged proteins on colloidal particles can alter the particle deposition on a glass substrate.[52] The amount of the adsorbed protein and the charge on the original colloidal particles affect the electrostatic interactions between the particles and the substrate in a similar way as described above and correspondingly alter the final deposition structures (Figure 1e).

Anyfantakis and coworkers studied the influence of the particles' hydrophobicity on the deposit morphology.[53] The surface wettability of silica nanoparticles was controlled by the reaction of the silanol group with dichlorodimethylsilane. On the basis of the hydrophobicity and concentration of nanoparticles in the suspension, the particle deposition varied from a ring-like to a dome-like shape. Whereas most hydrophilic particles always tend to deposit along the droplet periphery, the hydrophobic particles tend to lump in the center of the droplet. The variation in deposit morphology is attributed to the particle−particle interactions determined by the surface chemistry of the colloidal particles. The interparticle interactions were repulsive due to the negative charges on the nonmodified nanoparticles (100% SiOH). However, decreasing the SiOH groups weakened the particle−particle electrostatic repulsion that generated dome-like morphologies as a result of the hydrophobic particle−particle interactions. The authors also pointed out that the gel transition played an important role in their system, which contributed to the dome-like deposition of hydrophobic particles under high solid concentrations. A similar gelation strategy has been utilized in limiting the evaporation-induced flow to change the particle deposition.[22]

Kim et al. investigated the influence of binary solvent mixture, surface-active surfactant, and surface-adsorbed polymer on the final deposition pattern.[54] The motivation behind this study was to identify the mechanism of the uniform particle deposition left after drying whisky droplets and to replicate its uniform deposition using controlled sessile droplets. Whisky is an ethanol/water mixture with diverse dissolved molecules. Different flow behaviors were recorded as the whisky droplet evaporated and organized as follows: (i) chaotic mixing, (ii) radially outward flow along the air−liquid interface and radially inward flow along the substrate, (iii) radially outward flow along the substrate and radially inward flow along the air−liquid interface, and (iv) outward capillary flow in the final stages of solvent evaporation (Figure 1f). To mimic the flow patterns of a drying whisky droplet, an ethanol/water mixture (35:65 wt %) was used as a solvent. The flow patterns of (i) and (ii) were obtained due to the solutal Marangoni flow; however, the absence of the last two flow patterns resulted in the failure in the formation of uniform particle depositions. The notion behind the uniform particle deposition obtained from drying whisky droplets is the natural phospholipids (natural surfactant) and natural polymers (i.e., lignin and polysaccharides). Introducing sodium dodecyl sulfate (SDS) to the ethanol/water mixture helped to replicate the same flow patterns observed in evaporating whisky droplets. Solutal and surfactant Marangoni flows were observed during the drying process because of the higher ethanol evaporation rate, followed by the SDS accumulation at the edge of the sessile droplet. Although the flow patterns of evaporating whisky droplets were mimicked by introducing SDS surfactant to the ethanol/water binary mixture, the particle deposition was not uniformly distributed on the substrate. This issue was addressed by adding poly(ethylene oxide) (PEO) polymer that resembled the natural polymers in whisky droplets, which assisted the adherence of the suspended particles to the substrate (Figure 1g).

DOI: 10.1021/acs.jpcc.9b00797
J. Phys. Chem. C 2019, 123, 12029−12041

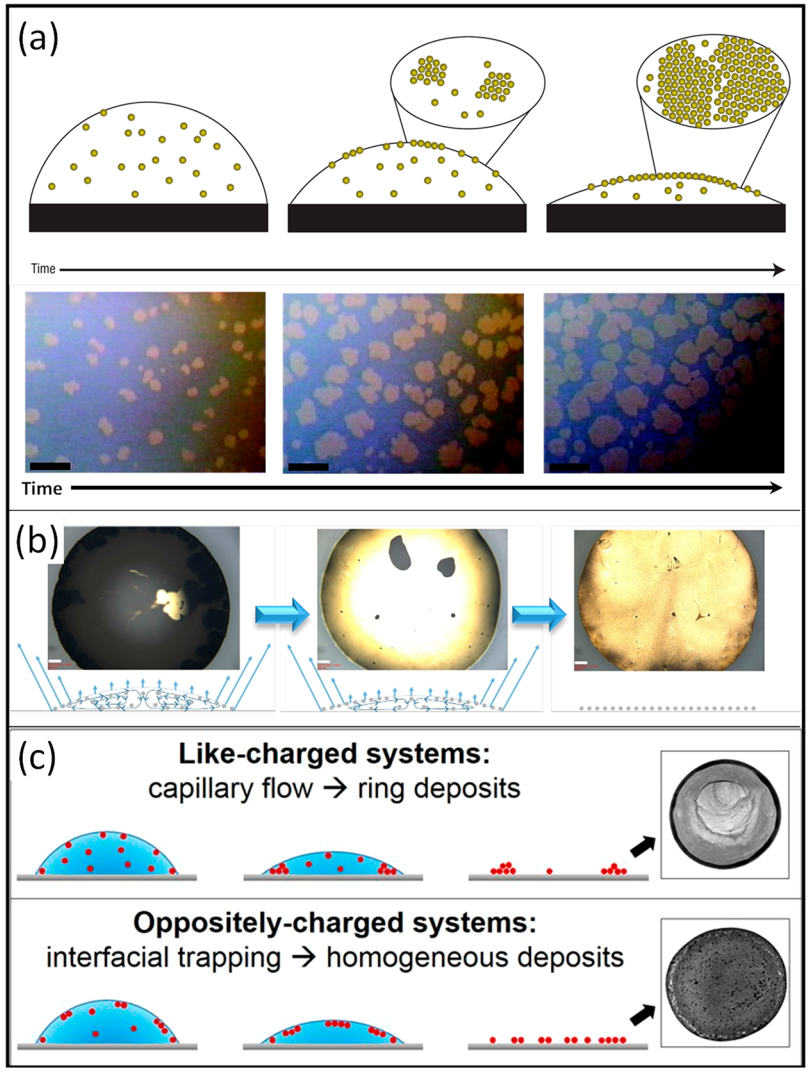

Figure 2. (a) Illustration of the particle self-assembly at the air−liquid interface during solvent evaporation (top row). The second row is the optical images showing the monolayer island formation of dodecanethiol-passivated gold nanocrystals at the interface during the evaporation process. Scale bars are 50 μm. Reprinted with permission ref 65. Copyright 2006 Springer Nature. (b) Optical images showing the self-assembly of thiol-capped Ga−In nanoparticles at the air−liquid interface in a cosolvent system (water/ethanol mixture), presented in different stages of solvent evaporation. Reprinted with permission from ref 66. Copyright 2016 American Chemical Society. (c) Schematic illustration of the surfactant-mediated electrostatic and hydrophobic interactions among the particles and the air−liquid and liquid−substrate interfaces. For a system with like-charged particle/surfactant mixtures, a ring-like particle deposition was obtained after the solvent completely evaporated. However, uniform particle deposits were obtained when utilizing oppositely charged systems. Reprinted with permission from ref 67. Copyright 2015 American Chemical Society.

3. PARTICLE ASSEMBLY AT THE AIR−LIQUID INTERFACE

Self-assembled monolayer films of colloidal particles are excellent candidates for the fabrication of functional coatings and devices.[55,56] The recent advances in colloidal particle deposition from the air−liquid interface have mitigated or suppressed the CRE and demonstrated highly ordered monolayer assembly of the deposition structures. This provides an excellent opportunity in the fabrication of functional coatings and devices through liquid processing. Because the particles are adsorbed and assembled at the interface, this self-assembly process does not involve particle−substrate interactions until the last stage of evaporation. Therefore, it is suitable for a wide variety of substrates, reducing the dependence on the chemical and physical homogeneity of the substrates.

Several factors contribute to the self-assembly process of colloidal particles adsorbed at the air−liquid interface such as capillary, van der Waals, and electrostatic forces.[57] The latter two interactions are included in the DLVO forces. Perhaps the most important particle−particle interaction at the interface is the lateral capillary force initiated by interfacial deformation.[58−61] The basic concept behind this interaction is minimizing the interfacial deformation energy that is greatly affected by the particle's size, shape, and wetting property. Floatation forces (originated by gravity and buoyancy) and immersion forces (due to the wetting properties of the particles) induce interfacial deformation around the particles. The capillary interaction between these particles can be attractive or repulsive, depending on whether the overlapping interfacial deformations around the two particles are analogous.[58−61] Monodisperse particles with similar wetting properties result in attractive capillary interactions at the air−liquid interface. Similarly, strong and long-ranged capillary attractions have been reported for ellipsoidal particles at an oil−water interface,[62] which can be approximately

DOI: 10.1021/acs.jpcc.9b00797
J. Phys. Chem. C 2019, 123, 12029−12041

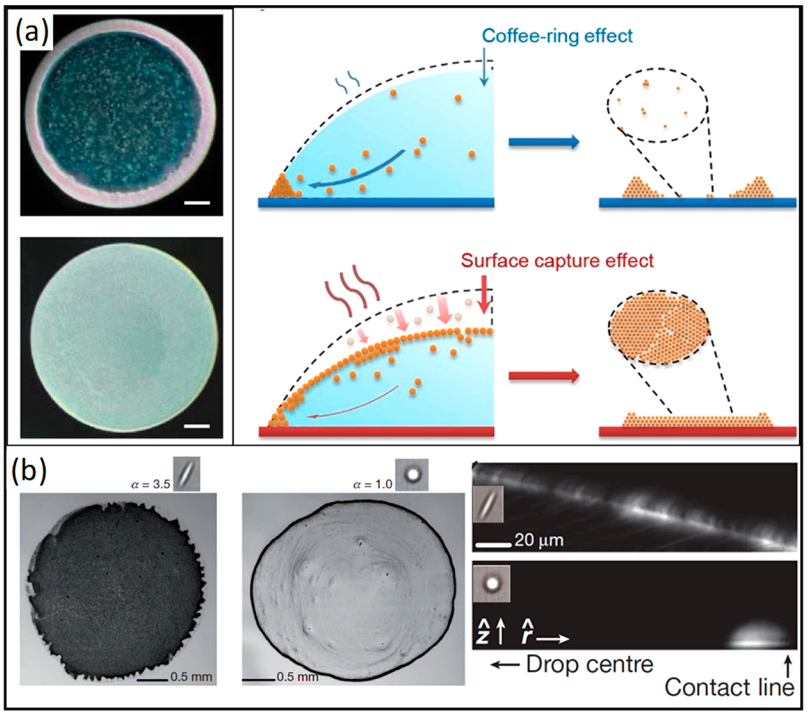

Figure 3. (a) Ring formation of colloidal droplets dried at room temperature versus uniform particle deposition of evaporating the same colloidal system in an environmental chamber at an elevated temperature. The colloidal particles were captured by the fast descending interface, forming uniform particle deposition. Scale bars are 0.5 mm. Reprinted from ref 71 under the Creative Commons license. (b) Effect of particle shape on the particle deposition. Reprinted with permission from ref 14. Copyright 2011 Springer Nature. The ellipsoidal particles tend to adsorb at the air−liquid interface during the evaporation, resulting in uniform depositions, as opposed to the ring-like deposition of spherical particles. The confocal microscope images shown on the right demonstrate the adsorption of the ellipsoidal particle at the air−liquid interface and the accumulation of the spherical particles at the contact line.

two orders of magnitude stronger than their spherical counterparts.[63] In addition, surface curvature also plays a critical role in the capillary assembly.[64]

When the particles adsorb at the interface, they experience the capillary attraction (in most cases) along with the DLVO forces to form self-assembled structures at the interface. In this section, we will review different routes of delivering colloidal particles to the air−liquid interface.

3.1. Particles Pushed to and Adsorbed at the Interface. Bigioni and coworkers formed monolayer depositions of dodecanethiol-ligated gold nanoparticles in toluene by pushing them to the air−liquid interface of the sessile droplets.[65] Direct, real-time, and real-space observations of the self-assembly of colloidal particles have been observed on the air−liquid interface during the solvent evaporation process. The nucleation and growth of the monolayer islands of gold nanoparticles were controlled via evaporation kinetics and particle−interface interactions. The mechanism of such a self-assembly process requires two key steps: (i) Rapid solvent evaporation segregates the colloidal particles near the air−liquid interface, where the interface descending velocity must be higher than the diffusion velocity of the colloidal particles. (ii) Once the colloidal particles reach the interface, the attractive particle−particle capillary interactions facilitate the network formation with exceptional long-range ordering (Figure 2a). The monolayer formation at the air−liquid interface was found to be highly dependent on the excess amount of dodecanethiol ligand in the system, where no nucleation or growth of gold islands was observed when the system was cleaned of excess dodecanethiol and vice versa. Although the details of the underlying mechanism were not unveiled in the original paper, it is hypothesized that the hydrophobic dodecanethiol-functionalized gold particles play a critical role in pushing the particles to the interface and forming the floating islands through self-assembly.

Boley and coworkers demonstrated a hybrid self-assembly of thiol-capped Ga−In particles using a cosolvent system (a mixture of ethanol/water).[66] The cosolvent in the sessile droplet segregated during the solvent evaporation, resulting in a concentrated shell of the solvent with high vapor pressure (ethanol) near the droplet interface and a water-enriched core. Consequently, the suspended particles, being hydrophobic and more stable in ethanol, favored to transport toward the air−liquid interface. Once the particles were carried to the surface of the droplet, they self-assembled into orderly monolayer films due to the particle−interface interactions (Figure 2b).

Anyfantakis et al. studied the influence of surfactant-mediated interactions on the particle deposition morphology.[67] Introducing surfactant to the system affected the particle−particle, particle−interface, and particle−substrate electrostatic and hydrophobic interactions, which dictated the final deposit morphology. Such interactions were modulated based on the surfactant type and concentration, charges on the particles, and the substrate. When the colloidal particles possessed surface charges similar to the polarity of the surfactant available in the system, a ring-like particle deposition was always the case. However, introducing surfactants with opposite charges of the colloidal particles generated different outcomes, where different particle deposit morphologies have been reported, ranging from ring-like to disk-like deposits. In this case, intermediate surfactant concentrations resulted in lower absolute zeta

DOI: 10.1021/acs.jpcc.9b00797
J. Phys. Chem. C 2019, 123, 12029−12041

potential values and higher particle hydrophobicity, leading to homogeneous particle depositions. In addition, some of the colloidal particles were noticed to adsorb at the air−liquid interface, forming a skin of colloidal particles during the evaporation process (Figure 2c). In contrast, higher surfactant concentrations resulted in charge reversal of the colloidal particles by which the ring-like deposits were retrieved. Similar ring-like particle depositions were observed at low surfactant concentrations.

Zhang et al. examined the self-assembly of thiolated single-stranded DNA-functionalized Au nanoparticles (ssDNA-AuNPs) at the vapor−solution interface by manipulating salt concentrations.[68] Although the interfacial assembly did not occur in an evaporating droplet, this work introduced some interesting mechanisms driving the colloidal particles to the interface. A trough containing the colloidal suspension with various salt concentrations was placed inside a sealed chamber to monitor the self-assembly process using liquid surface X-ray scattering. Whereas the hydrophobic nature of the nanoparticles facilitated the particle transport to the interface, the assembly and crystallization process were influenced by the critical salt concentration as a result of charge screening of the DNA. A similar observation has been reported when manipulating the pH and salt concentration of colloidal suspensions containing AuNPs functionalized with alkylthiol-terminated poly(acrylic acid) (PAA).[69]

Anyfantakis et al. also reported the possibility of colloidal particle adsorption and network formation at the air−liquid interface. Surfactant concentrations below the critical micelle concentration (CMC) enhanced the particle adsorption and assembly without significantly affecting the surface charge and wetting properties.[70] The particle adsorption was attributed to the preferential adsorption of the surfactant to the interface, which reduced the energy barrier between the interface and the like-charged particles. This facilitated the adsorption of particles at the interface. The author also commented on the degree of the packing and the arrangement of particles at the interface influenced by particle and surfactant concentrations. However, because the assembly process is much slower compared with typical droplet evaporation, it was not applied to evaporating droplets in this work. Interested readers can refer to the article for more details.

3.2. Particles Captured by the Descending Air−Liquid Interface. Li and coworkers proposed a different mechanism to suppress the CRE through capturing and self-assembling the colloidal particles onto the rapidly descending air−liquid interface.[71] Evaporation of the colloidal droplet was performed in an environmental chamber with a constant temperature and humidity. Elevating the evaporation temperature reduced the number of particles deposited at the periphery of the evaporative sessile droplet, producing more uniform particle deposition (Figure 3a). On the contrary, if the same colloidal droplets were left to dry under normal conditions, then a ring-like structure could evolve, especially when the contact lines remained pinned. This behavior was explained by the particle adsorption and assembly at the descending interface. At a sufficiently high evaporation temperature, the descending rate of the air−liquid interface is faster than the diffusion rate of the colloidal particles returning to the bulk, which facilitates capturing the neighboring particles by the interface. In this case, the particle jam at the interface increases the surface viscosity much higher than that of the bulk to resist the outward capillary flow, leading to more uniform particle deposition. The author also reported that transitional particle deposition composed of the particles that accumulated at the edge of the deposit along with the particles that adsorbed at the interface could be obtained at moderate evaporation temperatures.

Changing the particle shape is another approach proposed for eliminating the CRE, where elongated particles have been observed to adsorb at the air−liquid interface during the solvent evaporation process. Yunker and coworkers proved experimentally that the particle anisotropy is a crucial factor in determining the uniformity of particle depositions during the solvent evaporation process.[14] Polystyrene particles were stretched asymmetrically to different aspect ratios and dispersed in water. Then, the colloidal droplets were left to dry on a glass slide. Whereas spherical or slightly deformed (aspect ratio α = 1 to 1.1) colloidal particles were efficiently transported to the contact line by the evaporative-driven capillary flow, ellipsoidal particles with aspect ratio α > 1.1 were deposited uniformly during solvent evaporation. In a similar fashion as their spherical counterparts, the ellipsoidal particles were entrained to the edge of the sessile droplet by virtue of the outward capillary flow until they were caught by the descending air−liquid interface. Once the particles were captured by the interface, they experienced strong long-ranged interparticle attraction forces, forming loosely packed arrested structures at the interface (Figure 3b). Additionally, the adsorption of ellipsoidal particles to the interface increases the local viscosity, which resists the outward capillary flow. Spherical colloidal particles, however, were desorbed from the interface back to the bulk of the droplet due to much weaker interparticle attraction forces than those of ellipsoidal particles. The author also demonstrated that mixing ellipsoidal particles with spherical ones helped suppress the ring formation, where the spherical particles joined the assembled structure, producing a uniform particle deposition. Kim et al. further elaborated on the interparticle capillary force and the hydrodynamic force exerted on the ellipsoidal particles using an analytical model.[72] When the capillary force is greater than the hydrodynamic force, the ellipsoids form a stable network at the interface, inhibiting their migration to the contact line. On the contrary, when the hydrodynamic force is greater than the capillary force, the particles cannot remain at the interface; instead, they are transported to the contact line under the dominating hydrodynamic force. The experiments agreed reasonably well with the analytical analysis. No such adsorption of ellipsoidal particles at the air−liquid interface was reported when surfactant was introduced to the system due to the decrease in the surface tension of the droplet and lowering of the interface deformation energy.[14]

Dugyala and Basavaraj investigated the charge effect of colloidal hematite ellipsoids on the interfacial adsorption and the final particle deposition. pH modulation and the DLVO interactions have been adopted to tune the charge and zeta potential of the ellipsoids.[13] A similar general trend has been observed, as in the work of Bhardwaj et al.; that is, ring formation occurred for extreme acidic and basic conditions, whereas uniform deposition was observed for the intermediate pH levels (pH 6.5 and 8).[51] However, Dugyala and Basavaraj attributed the uniform deposition to the adsorption of particles at the interface due to the weakened image charge effect in the low dielectric medium (air). This hypothesis was partially supported by the fact that the ellipsoidal hematite particles adsorbed to the surface of a pendant droplet in a decane medium under intermediate pH conditions, whereas no particle adsorption occurred in extreme acidic solutions. The colloidal droplet was

DOI: 10.1021/acs.jpcc.9b00797
J. Phys. Chem. C 2019, 123, 12029−12041

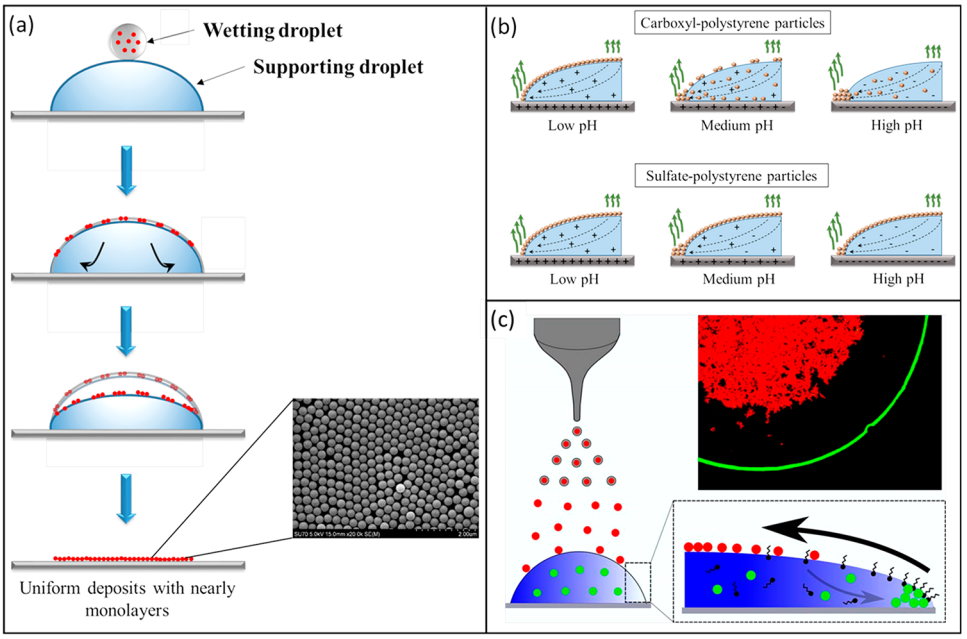

Figure 4. (a) Schematic of dual-droplet printing, where the wetting droplet spreads over the interface of the supporting droplet. Reprinted with permission from ref 73. Copyright 2018 John Wiley and Sons. The colloidal particles self-assemble on the interface, forming a network of particles that eventually produces a uniform, closely packed particle deposition after solvent evaporation. (b) Illustration of the multibody interactions at different pH values of the supporting droplet. Reprinted with permission from ref 74. Copyright 2018 Elsevier. The positive and negative signs represent the ions available in the supporting droplet at various pH values. (c) Illustration of the direct delivery of colloidal particles to the air–liquid interface by electrospray. Reprinted with permission from ref 75. Copyright 2018 American Chemical Society.

suspended in the decane medium to avoid the solvent evaporation. This also showcases the complexity of the multibody interactions involved in the evaporation of colloidal particles on a solid substrate.

3.3. Particles Directly Deposited and Spread on the Interface. All the work on the particle interfacial assembly discussed so far involved particle-laden sessile droplets and the colloidal particles adsorbed onto the interface driven by various means, for example, hydrophobic functionalization, particle shape, particle charge, solvent system, evaporation rate, and so on. By transforming the Langmuir–Blodgett (LB) concept to the picoliter droplets, we have recently proposed an alternative concept to self-assemble the nanoparticles at the air–liquid interface through a dual-droplet inkjet printing process.[73] The deposition of monolayer nanoparticle films is achieved by consecutively printing a supporting droplet and wetting droplets (Figure 4a). The colloidal particles spread over the supporting droplet surface and assemble on the interface as the solvent dries to produce a uniform, nearly monolayer deposition of nanoparticles. When the wetting droplet impacts and spreads on the supporting droplet, the colloidal particles experience various types of interactions such as particle–interface and particle–particle interactions, where the capillary forces compete with the particle electrostatic interactions and the particles' water affinity at the interface to facilitate the skin formation of nanoparticles. Three main steps take place during the monolayer self-assembly: (i) spreading of the wetting droplet and colloidal nanoparticles over the supporting droplet, (ii) nanoparticle packing and assembly on the interface between the wetting droplet and supporting droplet, and (iii) settling of the nanoparticle film layer onto the substrate upon the evaporation of the supporting droplet. The spreading of the wetting droplet is enabled by formulating a low-surface-tension ink containing colloidal particles and a high-surface-tension solvent for the supporting droplet. Deionized (DI) water was used as the solvent for supporting droplets; a mixture of ethanol/water was used as the solvent for wetting droplets. Monodispersed polystyrene (PS) nanoparticles with different surface functionalization and charge density were used as the colloidal particles.

The spreading of the wetting droplet and colloidal particles at the interface has been verified through high-speed imaging. The final destination of the colloidal particles, however, differs depending on the solvent composition of the wetting droplets, the particle charge density, and the amount of PS nanoparticles deposited onto the supporting droplet. When using pure ethanol as a solvent for the wetting droplet and particles with less surface charge density, the jetted colloidal particles can self-assemble into a particle film layer at the air–liquid interface of the supporting droplet, which is transferred to the substrate after the solvent is completely evaporated. This leads to a nearly monolayer and closely packed particle deposition. On the contrary, as a result of changing the wetting droplet solvent composition or increasing the surface charge density, some nanoparticles get trapped at the interface until the final deposition onto the substrate, and some may desorb from the interface and diffuse into the bulk of the supporting droplet during the solvent evaporation process.

The pH modulation of the supporting droplet resulted in different particle depositions.[74] The self-assembly process is strongly influenced by the protonation and deprotonation of the supporting droplet, which, in turn, controls the surface charge magnitude of the particles at the interface (Figure 4b). The final structure of the particle assembly is determined by the particle's affinity to water (type of functional groups and density), the charge level of the PS particles (zeta potential), and the pH of the supporting droplet. Consequently, controlling these experimental conditions resulted in different particle deposi-

DOI: 10.1021/acs.jpcc.9b00797
J. Phys. Chem. C 2019, 123, 12029–12041

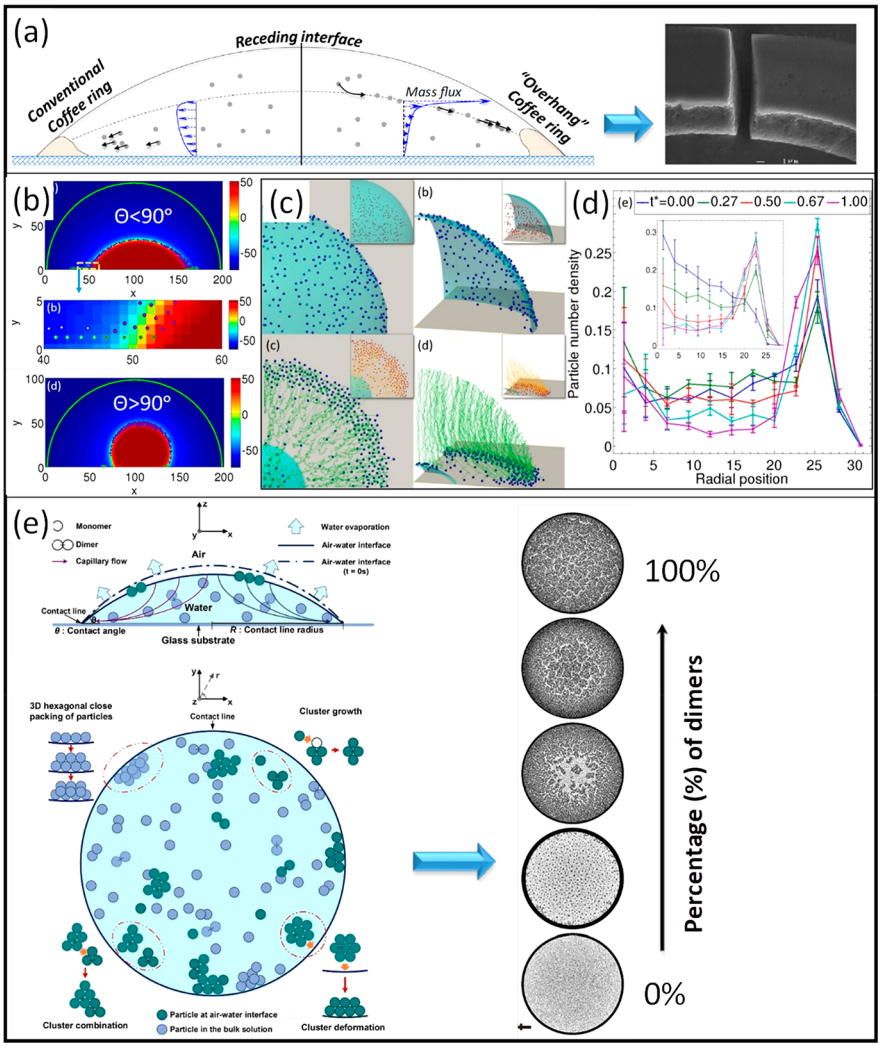

Figure 5. (a) Illustration of the critical boundary line that determines the fate of the colloidal particles at the interface or in the bulk of the droplet. Reprinted with permission from ref 82. Copyright 2017 Elsevier. An overhang ring structure is observed when the majority of the migrated colloidal particles are located close to the air−water interface (i.e., above the boundary line). (b) Simulation results showing the particle distribution at the air−liquid interface for evaporating sessile droplets with different contact angles. Reprinted with permission from ref 83. Copyright 2017 American Chemical Society. (c) Top and side views of interface-bound particles displayed at the beginning and at the end of solvent evaporation and (d) simulated particle deposition at different stages of evaporation. Reprinted with permission from ref 84. Copyright 2018 American Physical Society. (e) Illustration of the discrete element model of an evaporating sessile droplet with spherical monomers (single microspheres) and nonspherical dimers (pairs of monomers). The particle depositions shown on the right are highly dependent on the number of dimers available in the system. Reprinted from ref 85 under the Creative Commons license.

tions ranging from nearly monolayer, fully covered, closely packed depositions with no CRE to uniform monolayer particle depositions with particle accumulation at the ring and particle deposition with the conventional CRE.

A similar technique to directly deliver particles to the air−liquid interface by the electrospray technique has been demonstrated by Ghafouri and coworkers.[75] When the distance between the electrospray nozzle tip and the target droplet was sufficiently large, the generated spray (e.g., solvent-encapsulated nanoparticles) completely evaporated while in flight. This was to ensure the delivery of dry nanoparticles to the target droplet, enhancing the particle adsorption on the air−liquid interface. The interface was covered with nanoparticles when surfactant-free suspension was utilized, resulting in uniform, loosely packed particle depositions. This was attributed to the lack of surface flow at the air−liquid interface. A similar observation was reported when electrospraying the colloidal suspension with a high-molecular-weight surfactant. Conversely, introducing a low-molecular-weight surfactant to the spraying solution affected the particle assembly at the interface. In this case, the particles aggregated at the apex of the target droplet during the solvent evaporation process, resulting in a high-density region at the center of the final deposit (Figure 4c). The authors explained this behavior as desorption of the low-molecular-weight surfactant to the bulk of the target droplet, where the surfactant accumulation at the edge of the droplet generated the solutal Marangoni flow that forced the particles to aggregate at the apex of the droplet.

4. SIMULATION OF PARTICLE DYNAMICS AND ASSEMBLY AT THE INTERFACE

Besides the extensive experimental research efforts dedicated to provide a better understanding of the evaporation-driven self-assembly and deposition of colloidal suspensions, analytical

DOI: 10.1021/acs.jpcc.9b00797
J. Phys. Chem. C 2019, 123, 12029−12041

solution and numerical simulation of evaporating sessile droplets are indispensable tools for gaining more insight into the colloidal particle dynamics and their relationship to particle deposition patterns.[51,76−80] This Review Article focuses on the simulation work involving interfaces and particle−interface interactions.

The general consensus is that the ring of particles at the contact line, formed during the evaporation of colloidal suspensions, is driven by the evaporation-induced flow in the bulk of the droplet to the contact line. However, Jafari Kang et al. proposed an alternative mechanism to the coffee-ring formation: The evaporation-induced flow inside the droplet drives the particles to the descending interface; as the particles are captured by the air−liquid interface, they transport along the interface to the three-phase contact line.[81] The capture of the particles by the interface was supported by Lagrangian tracing of particles driven by the evaporation-induced flow and modeled as a 1D advection process. The velocity of the transported particles was assumed to be the same as the flow velocity, where the particle diffusion and thermal Marangoni flow were neglected in the mathematical model. The interfacial transport was considered to be the only mechanism to determine the final deposition structure. The author found that the fraction of the particles captured at the interface was almost identical to the droplet volume loss due to evaporation. At the completion of solvent drying, no particles had deposited onto the substrate before reaching the air−liquid interface because the fluid velocity tends to zero when approaching the substrate, and the model did not consider any particle−substrate interactions. Regardless the contact angles utilized in the model, the final particle distribution was similar, where the particles accumulated at the contact line region, forming the ring-like depositions. This work has pioneered the involvement of the air−liquid interface in modeling an evaporating particle-laden droplet and the prediction of the particle deposition. Nonetheless, this model lacks the consideration of critical interactions, such as, particle−substrate and particle−particle interactions.

Different from Jafari Kang and Masoud's model, where all the particles reached the air−liquid interface before they deposited onto the substrate,[81] Nguyen and coworkers examined the competition between the colloidal particles remaining in the bulk of the droplet following the evaporation-induced convective flow, and the particles reached and adsorbed at the air−liquid interface before they deposited onto the solid substrate.[82] The Lagrangian modeling approach was utilized to track the particles inside and at the interface of the evaporative droplet, where the particles were assumed to move toward the solid substrate in a non-Brownian motion, influenced by drag force (particle−flow-field interaction), colloidal forces (particle−substrate and particle−interface interactions) based on the DLVO theory, and gravitational forces. In the mathematical model, the authors considered a pinned three-phase contact line during the evaporation process. The results revealed a boundary line in the evaporating droplet that divided the colloidal particles into two groups, above which the colloidal particles were carried to and captured by the air−liquid interface and below which the colloidal particles remained in the droplet and followed the evaporation-induced convective flow (Figure 5a). Eventually all of these particles deposited onto the substrate, forming a ring-like structure. An "overhang" structure identified in the ring of colloidal SiO_2 particle deposits supported the model prediction that a significant fraction of the particles transport along the interface or near the interface, contributing to the ring formation at the contact line. The authors also studied the effect of the evaporation rate, the residence time of particles in the bulk of the droplet, and the particle capture efficiency.

Nguyen's model allows quantitative comparison of the roles of particle−substrate and particle−interface interactions. However, as the authors pointed out, caution needs to be taken in predicting the final particle deposition because the particle tracking was stopped when it reached either the substrate or the interface. In reality, particles can desorb from the interface back to the bulk of the droplet or self-assemble into monolayer films floating at the interface, depending on the particle hydrophobicity, surface charge density, and so on, as reviewed in the previous sections.

In 2017, Zhao and Yong investigated the particle deposition of evaporative sessile droplets using the lattice Boltzmann simulation. In particular, they studied how the surface flow of evaporating droplets affects the deposition of particles adsorbed at the interface for depinned contact lines (i.e., constant contact angle).[83] Their model utilized a free-energy-based, two-way coupled lattice Boltzmann−Brownian dynamics (LB−BD) method to simulate 3D particle-laden droplets under isothermal, quasi-steady evaporation conditions. During the solvent evaporation, the interfacial particles accumulated around the contact line areas for a contact angle <90°. In contrast, the droplet with a contact angle >90° had a higher particle concentration at the apex of the droplet (Figure 5b). This redistribution of the interfacial particles can be attributed to the evaporation-induced advection flow with moving contact lines, where a surface flow is generated in the former case, pointing to the contact line, and in the latter case, the surface flow is pointing to the apex. Final particle deposits formed from the particles in the bulk exhibited a dome shape due to the depinned contact line. On the contrary, the deposit of the interfacial particles showed a larger deposition footprint because the interfacial particles deposit onto the substrate under particle−substrate interactions. For a contact angle of 60°, two peaks were formed at the deposition edge due to the surface flow toward the contact line.

The authors also compared the interface flow and final deposition of both particles from the bulk and at the interface for a pinned contact line.[84] A typical ring-like deposition has been obtained from the droplet with particles in the bulk driven by the evaporation-induced flow. Droplets with interfacial particles, on the contrary, exhibited a small enhancement in the number of particles at the center of the deposit along with a pronounced CRE structure (Figure 5c,d). The descending interface displacement contributes to the particle migration toward the droplet apex in an earlier and shorter phase, whereas the dominant interface flow drives the interfacial particles to the contact line, especially in the last stage of evaporation, forming CRE deposits.

This modeling work has provided critical and valuable hydrodynamic insight into the assembly of interface-bounded particles. However, one critical aspect about the colloidal particles might be missing; that is, the cluster assembly (small monolayer islands of particles at the interface) demonstrated in many experimental works[65,66,73,74] has not been considered in this model. These monolayer clusters float and move at the interface as entities, possibly with different dynamics. In addition, the particles were assumed as point masses without physical volumes, which may require some caution in predicting the final particle deposition.

DOI: 10.1021/acs.jpcc.9b00797
J. Phys. Chem. C 2019, 123, 12029−12041

In 2017, Xu et al. studied the interfacial assembly in an evaporating droplet using a discrete element model, considering cluster assembly at the air−liquid interface.[85] On the basis of the observation that ellipsoid particles effectively suppress the CRE through interface adsorption,[14] this model has simulated the assembly of a combination of monomers (single spherical particles) and dimers (two spherical particles attached together as a surrogate for ellipsoid particles). The analytical solution of droplet evaporation and its resultant convective flow were incorporated into the model, and the particles were assumed to transport following the evaporation-induced flow and Brownian motion. The authors first verified the CRE formation when only monomers were used in the model. For a mixture of monomers and dimers in the system, cluster growth was initiated when a dimer reached and adsorbed at the air−liquid interface through recruiting other monomers at the interface (Figure 5e). Cluster combination and cluster deformation were also considered in the model. During the evaporation, various sizes of monolayer islands were self-assembled at the interface with hexagonal close-packing that effectively suppressed the CRE. A higher ratio of the dimers provided a stronger suppression effect, leading to more uniform depositions (Figure 5e).

The authors also studied the effect of a circulatory Marangoni flow on the particle deposition due to the temperature gradient from the center to the edge of the droplet. Surprisingly, the introduced thermal Marangoni flow did not enhance the cluster formation at the air−liquid interface; instead, it reduced the number of dimers reaching the interface under the inward and downward circulatory flow near the interface. This conclusion may not be applicable to the Marangoni flow induced by surface-active surfactants,[54] which is likely along the air−liquid interface.

It has been experimentally proven that particle−particle interactions at the air−liquid interface (DLVO forces, capillary forces, cluster assembly, etc.), particle−interface interactions or cluster−interface interactions (capillary forces), and particle−substrate interactions significantly affect the particle deposition. The modeling work involving air−liquid interfaces is still in its early stage, and such complexities are usually avoided or only partially considered when simulating evaporating colloidal droplets. However, it is necessary and critical to consider implementing these intricate interactions at the interface in future simulation work to fully comprehend the particle dynamics during the self-assembly and their impact on the final particle deposition.

5. DISCUSSION

Interfacial assembly has been extensively investigated for several decades, since the first demonstration of Langmuir−Blodgett films. This Review Article focuses on the particle interface assembly in evaporating sessile droplets. The evaporation of particle-laden droplets is an intricate process involving the above-mentioned multibody interactions. The conventional approaches to mitigate the CRE, for example, introducing Marangoni flow to bring the colloidal particles back to the center of the droplet or substrate treatment to enhance particle−substrate interactions, can produce relatively uniform and homogenized depositions but not a monolayer deposition. Well-ordered monolayer deposition of colloidal particles can be obtained by particle assembly at the air−liquid interface, where the particles adsorb and self-assemble to form monolayer "islands" or clusters trapped at the interface in an energetically favorable state. This is due to the interfacial deformation caused by the larger size and fractal shape of the particle agglomerates.

To promote the particle assembly at the air−liquid interface, at least one of the three key events must be adopted: (i) particles transport from the bulk and adsorb at the interface of the sessile droplets; (ii) the descending interface captures the particles; and (iii) particles initially spread and maintain at the interface of the sessile droplets. (Note: Reactive systems that can generate colloidal particles in situ are excluded from this discussion.) In the first category, particle transport to the interface has been realized through manipulating the particle−particle interaction (e.g., neutralization to facilitate particle agglomeration) and the particle−fluid interaction (e.g., hydrophobic particles and cosolvent system). The second category includes the fast evaporation of solvent or the utilization of anisotropic particles. Special considerations must be taken in matching the assembly kinetics and the rate of the descending interface to ensure sufficient time for the particle assembly at the interface before the solvent completely evaporates. The last category is represented by the dual-droplet printing. In dual-droplet printing, nanoparticle-laden wetting droplets are jetted over a supporting droplet. Upon the impact of the wetting droplet on the supporting droplet, the particles spread and assemble at the interface of the supporting droplet. At the air−liquid interface, the particles experience various types of interactions such as capillary attraction force and particle−particle DLVO force to facilitate the formation of a closely packed monolayer of colloidal particle assembly.

Compared with the particle interfacial assembly without involving evaporation (e.g., LB method), more stringent requirements need to be fulfilled for evaporating sessile droplets to generate well-ordered assembly structures. Ideally all of the colloidal particles in the sessile droplets reside and assemble at the interface through one of the three routes discussed above. Any particles in the bulk of the droplets will follow the evaporation-induced convective flow toward the contact lines, unless some other mechanisms change its course. Deposition of these particles would appear as defects in the orderly deposition generated by the interfacial assembly. Therefore, in terms of deposition quality or degree of orderliness, the third and the first categories maybe superior to the second category. In the third category, the proper particle properties (functional groups, surface charge, hydrophobicity, etc.) and dispensing conditions enable the direct spreading and self-assembly of the particles to form monolayer films at the interface. In this case, no particles would exist in the bulk of the sessile droplet when they remain self-assembled at the interface. However, in the second category, the particles are either being captured by the descending air−liquid interface or being carried to the contact line region by the evaporation-induced flow. Some particles may prematurely deposit onto the substrate (if they are close to the substrate) before being captured by the interface and assembled with other particles. The first category has the advantage that the particles tend to transport to the interface under certain driving forces, for example, hydrophobic interactions, solvent segregation, and so on, avoiding premature deposition onto the substrate. In all of these cases, the growth dynamics of the assembled clusters or "islands" into long-range ordered structures need to be further investigated.

In addition, the evaporation of the particle-covered droplets involves two-way interactions between evaporation and particle assembly. The evaporation reduces the interfacial surface area, which compresses the assembled clusters/films. As a result, more densely packed monolayer structures or locally crumpled, multilayer structures can be formed. Evaporation also induces a

DOI: 10.1021/acs.jpcc.9b00797
J. Phys. Chem. C 2019, 123, 12029−12041

radial surface flow at the interface, which tends to carry the assembled clusters/films toward the contact line. Alternatively, the presence of particles at the air−liquid interface may enhance the evaporation flux due to reduced surface tension,[83] slow down the evaporation rate due to the decreased accessible interfacial surface area,[86,87] or a combination of both at different stages of evaporation.

It is also worth pointing out that the particle deposition obtained by interfacial assembly may possess some ring structures at the contact line due to the evaporation-induced flow at the interface and particle−substrate interactions in the contact line region (e.g., electrostatic and van der Waals interactions). In particular, during the last stages of solvent evaporation, the particles at the interface may experience a "rush hour" effect.[84] Nevertheless, this ring formation can be mitigated by introducing a repulsive particle−substrate interaction (e.g., adjusting the pH of the sessile droplet).[74]

6. SUMMARY AND OUTLOOK

The evaporation of a particle-laden droplet and the formation of the particle depositions depend on many factors such as particles, solvent(s), environmental conditions, substrate roughness and wettability, and so on. Such evaporation phenomenon of the particle-laden sessile droplets on a solid substrate involves rich and profound physics and intricate multibody interactions. Despite the plethora of studies conducted in this field, a comprehensive understanding of this evaporative process and the patterns obtained after solvent evaporation is still inadequate, especially the new perspective of particle interfacial assembly.

This Review Article summarizes and highlights the recent advances in promoting the interfacial assembly to mitigate or completely suppress the CRE and to produce a well-ordered particle assembly. The self-assembly of colloidal particles has been widely recognized as a viable approach to generate a variety of nanostructures. It also holds great potential to be implemented in many engineering disciplines on different length scales. Despite the considerable advances, particle interfacial assembly in evaporating sessile droplets is still in its early stages. Future works of experimental, theoretical, and computational investigations should be conducted to promote a thorough understanding of the mechanisms behind the resultant particle assembly and deposition, for example, particle transport to the interface, assembly at the interface, two-way interactions between evaporation and assembled structures, packing order of the final assembled structures, and so on. Specifically, future directions in this field will likely include: (i) particle transport to the interface, especially when both droplet size and evaporation time decrease; (ii) comprehensive understanding of the kinetics of cluster nucleation at the interface, the cluster growth and compression of the assembled clusters/films on the interface during solvent evaporation, and the effect of interfacial hydrodynamic flow on the assembled structure; (iii) interfacial assembly of anisotropic particles (shape anisotropy, e.g., nanowires and nanosheets; composition anisotropy, e.g., Janus particles) and binary particles in an evaporating droplet; (iv) factors and mechanisms affecting the packing order and density of the final assembled structure; and (v) further exploration of potential applications. The well-ordered monolayer deposition enabled by particle interfacial assembly in evaporating droplets is a promising venue that holds great potential in the fabrication of functional coatings and optical and electronics devices.

AUTHOR INFORMATION

Corresponding Author

*Tel: (804) 827-7025. Fax: (804) 827-7030. Tel: hzhao2@vcu.edu.

ORCID

Hong Zhao: 0000-0001-9148-0158

Notes

The authors declare no competing financial interest.

Biographies

Karam Nashwan Al-Milaji is currently a Ph.D. graduate student in the Department of Mechanical and Nuclear Engineering at Virginia Commonwealth University (VCU). He completed his undergraduate studies in 2007 at Technical College of Mosul, Iraq, followed by 6 years of working as a maintenance engineer of heating, ventilation, and air conditioning (HVAC) systems. He earned his M.S. degree in the Department of Mechanical and Nuclear Engineering of VCU in 2016. His research focuses on inkjet printing of functional materials to investigate material interactions on different length scales.

Hong Zhao is currently an assistant professor in the Department of Mechanical and Nuclear Engineering at VCU. She received her B.S. and M.S. degrees in mechanical engineering from China University of Petroleum and her Ph.D. degree in mechanical and aerospace engineering from Rutgers University. Before joining VCU in 2014, she worked at Xerox Research Center Webster for about 8 years. Zhao's research interests include surface science and surface engineering, transport and self-assembly of colloidal nanoparticles, the development of printing processes (e.g., inkjet printing, electrohydrodynamic printing, direct extrusion printing, etc.), and printed functional devices.

ACKNOWLEDGMENTS

We are grateful for the support of the National Science Foundation (CMMI-1634938).

DOI: 10.1021/acs.jpcc.9b00797
J. Phys. Chem. C 2019, 123, 12029−12041

REFERENCES

(1) Mampallil, D.; Eral, H. B. A Review on Suppression and Utilization of the Coffee-Ring Effect. *Adv. Colloid Interface Sci.* **2018**, *252*, 38−54.
(2) Parsa, M.; Harmand, S.; Sefiane, K. Mechanisms of Pattern Formation from Dried Sessile Drops. *Adv. Colloid Interface Sci.* **2018**, *254*, 22−47.
(3) Anyfantakis, M.; Baigl, D. Manipulating the Coffee-Ring Effect: Interactions at Work. *ChemPhysChem* **2015**, *16*, 2726−2734.
(4) Deegan, R. D.; Bakajin, O.; Dupont, T. F.; Huber, G.; Nagel, S. R.; Witten, T. A. Capillary Flow as the Cause of Ring Stains from Dried Liquid Drops. *Nature* **1997**, *389*, 827−829.
(5) Deegan, R. D. Pattern Formation in Drying Drops. *Phys. Rev. E: Stat. Phys., Plasmas, Fluids, Relat. Interdiscip. Top.* **2000**, *61*, 475−485.
(6) Deegan, R. D.; Bakajin, O.; Dupont, T. F.; Huber, G.; Nagel, S. R.; Witten, T. A. Contact Line Deposits in an Evaporating Drop. *Phys. Rev. E: Stat. Phys., Plasmas, Fluids, Relat. Interdiscip. Top.* **2000**, *62*, 756−765.
(7) Sun, J.; Bao, B.; He, M.; Zhou, H.; Song, Y. Recent Advances in Controlling the Depositing Morphologies of Inkjet Droplets. *ACS Appl. Mater. Interfaces* **2015**, *7*, 28086−28099.
(8) Han, W.; Lin, Z. Learning from "Coffee Rings": Ordered Structures Enabled by Controlled Evaporative Self-Assembly. *Angew. Chem., Int. Ed.* **2012**, *51*, 1534−1546.
(9) Dugyala, V. R.; Basavaraj, M. G. Evaporation of Sessile Drops Containing Colloidal Rods: Coffee-Ring and Order-Disorder Transition. *J. Phys. Chem. B* **2015**, *119*, 3860−3867.
(10) Parsa, M.; Harmand, S.; Sefiane, K.; Bigerelle, M.; Deltombe, R. Effect of Substrate Temperature on Pattern Formation of Nanoparticles from Volatile Drops. *Langmuir* **2015**, *31*, 3354−3367.
(11) Chhasatia, V. H.; Joshi, A. S.; Sun, Y. Effect of Relative Humidity on Contact Angle and Particle Deposition Morphology of an Evaporating Colloidal Drop. *Appl. Phys. Lett.* **2010**, *97*, 231909.
(12) Majumder, M.; Rendall, C. S.; Eukel, J. A.; Wang, J. Y. L.; Behabtu, N.; Pint, C. L.; Liu, T. Y.; Orbaek, A. W.; Mirri, F.; Nam, J.; et al. Overcoming the "Coffee-Stain" Effect by Compositional Marangoni-Flow-Assisted Drop-Drying. *J. Phys. Chem. B* **2012**, *116*, 6536−6542.
(13) Dugyala, V. R.; Basavaraj, M. G. Control over Coffee-Ring Formation in Evaporating Liquid Drops Containing Ellipsoids. *Langmuir* **2014**, *30*, 8680−8686.
(14) Yunker, P. J.; Still, T.; Lohr, M. A.; Yodh, A. G. Suppression of the Coffee-Ring Effect by Shape-Dependent Capillary Interactions. *Nature* **2011**, *476*, 308−311.
(15) Davidson, Z. S.; Huang, Y.; Gross, A.; Martinez, A.; Still, T.; Zhou, C.; Collings, P. J.; Kamien, R. D.; Yodh, A. G. Deposition and Drying Dynamics of Liquid Crystal Droplets. *Nat. Commun.* **2017**, *8*, 15642.
(16) Das, S.; Dey, A.; Reddy, G.; Sarma, D. D. Suppression of Coffee-Ring Effect: Evaporation Driven Disorder to Order Transition in Colloidal Droplets. *J. Phys. Chem. Lett.* **2017**, *8*, 4704−4709.
(17) Li, Y. F.; Sheng, Y. J.; Tsao, H. K. Evaporation Stains: Suppressing the Coffee-Ring Effect by Contact Angle Hysteresis. *Langmuir* **2013**, *29*, 7802−7811.
(18) Mampallil, D.; Reboud, J.; Wilson, R.; Wylie, D.; Klug, D. R.; Cooper, J. M. Acoustic Suppression of the Coffee-Ring Effect. *Soft Matter* **2015**, *11*, 7207−7213.
(19) Eral, H. B.; Augustine, D. M.; Duits, M. H. G.; Mugele, F. Suppressing the Coffee Stain Effect: How to Control Colloidal Self-Assembly in Evaporating Drops Using Electrowetting. *Soft Matter* **2011**, *7*, 4954−4958.
(20) Zhou, C.; Han, J.; Guo, R. A Facile Strategy to Colloidal Crystals by Drying Condensed Suspension Droplets. *J. Colloid Interface Sci.* **2013**, *397*, 80−87.
(21) Sempels, W.; De Dier, R.; Mizuno, H.; Hofkens, J.; Vermant, J. Auto-Production of Biosurfactants Reverses the Coffee Ring Effect in a Bacterial System. *Nat. Commun.* **2013**, *4*, 1757.
(22) Talbot, E. L.; Yow, H. N.; Yang, L.; Berson, A.; Biggs, S. R.; Bain, C. D. Printing Small Dots from Large Drops. *ACS Appl. Mater. Interfaces* **2015**, *7*, 3782−3790.
(23) Marin, A.; Liepelt, R.; Rossi, M.; Kaehler, C. Surfactant-Driven Flow Transitions in Evaporating Droplets. *Soft Matter* **2016**, *12*, 1593−1600.
(24) Zhong, X.; Crivoi, A.; Duan, F. Sessile Nanofluid Droplet Drying. *Adv. Colloid Interface Sci.* **2015**, *217*, 13−30.
(25) Li, J.; Ye, F.; Vaziri, S.; Muhammed, M.; Lemme, M. C.; Östling, M. Efficient Inkjet Printing of Graphene. *Adv. Mater.* **2013**, *25*, 3985−3992.
(26) Kim, T. Y.; Amani, M.; Ahn, G. H.; Song, Y.; Javey, A.; Chung, S.; Lee, T. Electrical Properties of Synthesized Large-Area MoS_2 Field-Effect Transistors Fabricated with Inkjet-Printed Contacts. *ACS Nano* **2016**, *10*, 2819−2826.
(27) Nguyen, P. Q. M.; Yeo, L. P.; Lok, B. K.; Lam, Y. C. Patterned Surface with Controllable Wettability for Inkjet Printing of Flexible Printed Electronics. *ACS Appl. Mater. Interfaces* **2014**, *6*, 4011−4016.
(28) Liu, L.; Ma, S.; Pei, Y.; Xiong, X.; Sivakumar, P.; Singler, T. J. Regulation of the Deposition Morphology of Inkjet-Printed Crystalline Materials via Polydopamine Functional Coatings for Highly Uniform and Electrically Conductive Patterns. *ACS Appl. Mater. Interfaces* **2016**, *8*, 21750−21761.
(29) Finn, D. J.; Lotya, M.; Coleman, J. N. Inkjet Printing of Silver Nanowire Networks. *ACS Appl. Mater. Interfaces* **2015**, *7*, 9254−9261.
(30) de Gans, B.-J.; Duineveld, P. C.; Schubert, U. S. Inkjet Printing of Polymers: State of the Art and Future Developments. *Adv. Mater.* **2004**, *16*, 203−213.
(31) Wu, L.; Dong, Z.; Li, F.; Zhou, H.; Song, Y. Emerging Progress of Inkjet Technology in Printing Optical Materials. *Adv. Opt. Mater.* **2016**, *4*, 1915−1932.
(32) Gençer, A.; Schütz, C.; Thielemans, W. Influence of the Particle Concentration and Marangoni Flow on the Formation of Cellulose Nanocrystal Films. *Langmuir* **2017**, *33*, 228−234.
(33) Chen, R.; Zhang, L.; Zang, D.; Shen, W. Blood Drop Patterns: Formation and Applications. *Adv. Colloid Interface Sci.* **2016**, *231*, 1−14.
(34) Yakhno, T. Salt-Induced Protein Phase Transitions in Drying Drops. *J. Colloid Interface Sci.* **2008**, *318*, 225−230.
(35) Brutin, D.; Sobac, B.; Loquet, B.; Sampol, J. Pattern Formation in Drying Drops of Blood. *J. Fluid Mech.* **2011**, *667*, 85−95.
(36) Wong, T. S.; Chen, T. H.; Shen, X.; Ho, C. M. Nanochromatography Driven by the Coffee Ring Effect. *Anal. Chem.* **2011**, *83*, 1871−1873.
(37) Noguera-Marín, D.; Moraila-Martínez, C. L.; Cabrerizo-Vílchez, M. A.; Rodríguez-Valverde, M. A. Particle Segregation at Contact Lines of Evaporating Colloidal Drops: Influence of the Substrate Wettability and Particle Charge-Mass Ratio. *Langmuir* **2015**, *31*, 6632−6638.
(38) Monteux, C.; Lequeux, F. Packing and Sorting Colloids at the Contact Line of a Drying Drop. *Langmuir* **2011**, *27*, 2917−2922.
(39) Wen, J. T.; Ho, C. M.; Lillehoj, P. B. Coffee Ring Aptasensor for Rapid Protein Detection. *Langmuir* **2013**, *29*, 8440−8446.
(40) Gulka, C. P.; Swartz, J. D.; Trantum, J. R.; Davis, K. M.; Peak, C. M.; Denton, A. J.; Haselton, F. R.; Wright, D. W. Coffee Rings as Low-Resource Diagnostics: Detection of the Malaria Biomarker Plasmodium Falciparum Histidine-Rich Protein-II Using a Surface-Coupled Ring of Ni(II)NTA Gold-Plated Polystyrene Particles. *ACS Appl. Mater. Interfaces* **2014**, *6*, 6257−6263.
(41) Soltman, D.; Subramanian, V. Inkjet-Printed Line Morphologies and Temperature Control of the Coffee Ring Effect. *Langmuir* **2008**, *24*, 2224−2231.
(42) Tekin, E.; Smith, P. J.; Schubert, U. S. Inkjet Printing as a Deposition and Patterning Tool for Polymers and Inorganic Particles. *Soft Matter* **2008**, *4*, 703−713.
(43) Ooi, Y.; Hanasaki, I.; Mizumura, D.; Matsuda, Y. Suppressing the Coffee-Ring Effect of Colloidal Droplets by Dispersed Cellulose Nanofibers. *Sci. Technol. Adv. Mater.* **2017**, *18*, 316−324.
(44) Ding, Y.; Ling, J.; Qiao, Y.; Li, Z.; Sun, Z.; Cai, J.; Guo, Y.; Wang, H. A High-Throughput Fluorimetric Microarray with Enhanced Fluorescence and Suppressed "Coffee-Ring" Effects for the Detection of Calcium Ions in Blood. *Sci. Rep.* **2016**, *6*, 38602.

DOI: 10.1021/acs.jpcc.9b00797
J. Phys. Chem. C 2019, 123, 12029−12041

(45) Yen, T. M.; Fu, X.; Wei, T.; Nayak, R. U.; Shi, Y.; Lo, Y.-H. Reversing Coffee-Ring Effect by Laser-Induced Differential Evaporation. *Sci. Rep.* **2018**, *8*, 3157.
(46) Li, S.; Dong, M.; Li, R.; Zhang, L.; Qiao, Y.; Jiang, Y.; Qi, W.; Wang, H. A Fluorometric Microarray with ZnO Substrate-Enhanced Fluorescence and Suppressed "Coffee-Ring" Effects for Fluorescence Immunoassays. *Nanoscale* **2015**, *7*, 18453−18458.
(47) Baker, M. J.; Hussain, S. R.; Lovergne, L.; Untereiner, V.; Hughes, C.; Lukaszewski, R. A.; Thiéfin, G.; Sockalingum, G. D. Developing and Understanding Biofluid Vibrational Spectroscopy: A Critical Review. *Chem. Soc. Rev.* **2016**, *45*, 1803−1818.
(48) Lai, Y. H.; Cai, Y. H.; Lee, H.; Ou, Y. M.; Hsiao, C. H.; Tsao, C. W.; Chang, H. T.; Wang, Y. S. Reducing Spatial Heterogeneity of MALDI Samples with Marangoni Flows During Sample Preparation. *J. Am. Soc. Mass Spectrom.* **2016**, *27*, 1314−1321.
(49) Sefiane, K. Patterns from Drying Drops. *Adv. Colloid Interface Sci.* **2014**, *206*, 372−381.
(50) Yan, Q.; Gao, L.; Sharma, V.; Chiang, Y. M.; Wong, C. C. Particle and Substrate Charge Effects on Colloidal Self-Assembly in a Sessile Drop. *Langmuir* **2008**, *24*, 11518−11522.
(51) Bhardwaj, R.; Fang, X.; Somasundaran, P.; Attinger, D. Self-Assembly of Colloidal Particles from Evaporating Droplets: Role of DLVO Interactions and Proposition of a Phase Diagram. *Langmuir* **2010**, *26*, 7833−7842.
(52) Devineau, S.; Anyfantakis, M.; Marichal, L.; Kiger, L.; Morel, M.; Rudiuk, S.; Baigl, D. Protein Adsorption and Reorganization on Nanoparticles Probed by the Coffee-Ring Effect: Application to Single Point Mutation Detection. *J. Am. Chem. Soc.* **2016**, *138*, 11623−11632.
(53) Anyfantakis, M.; Baigl, D.; Binks, B. P. Evaporation of Drops Containing Silica Nanoparticles of Varying Hydrophobicities: Exploiting Particle-Particle Interactions for Additive-Free Tunable Deposit Morphology. *Langmuir* **2017**, *33*, 5025−5036.
(54) Kim, H.; Boulogne, F.; Um, E.; Jacobi, I.; Button, E.; Stone, H. A. Controlled Uniform Coating from the Interplay of Marangoni Flows and Surface-Adsorbed Macromolecules. *Phys. Rev. Lett.* **2016**, *116*, 124501.
(55) Ma, H.; Hao, J. Ordered Patterns and Structures via Interfacial Self-Assembly: Superlattices, Honeycomb Structures and Coffee Rings. *Chem. Soc. Rev.* **2011**, *40*, 5457−5471.
(56) Hou, J.; Li, M.; Song, Y. Patterned Colloidal Photonic Crystals. *Angew. Chem., Int. Ed.* **2018**, *57*, 2544−2553.
(57) Lotito, V.; Zambelli, T. Approaches to Self-Assembly of Colloidal Monolayers: A Guide for Nanotechnologists. *Adv. Colloid Interface Sci.* **2017**, *246*, 217−274.
(58) Kralchevsky, P. A.; Nagayama, K. Capillary Interactions Between Particles Bound to Interfaces, Liquid Films and Biomembranes. *Adv. Colloid Interface Sci.* **2000**, *85*, 145−192.
(59) Kralchevsky, P. A.; Denkov, N. D. Capillary Forces and Structuring in Layers of Colloid Particles. *Curr. Opin. Colloid Interface Sci.* **2001**, *6*, 383−401.
(60) Loudet, J. C.; Alsayed, A. M.; Zhang, J.; Yodh, A. G. Capillary Interactions Between Anisotropic Colloidal Particles. *Phys. Rev. Lett.* **2005**, *94*, 018301.
(61) McGorty, R.; Fung, J.; Kaz, D.; Manoharan, V. N. Colloidal Self-Assembly at an Interface. *Mater. Today* **2010**, *13*, 34−42.
(62) Loudet, J. C.; Yodh, A. G.; Pouligny, B. Wetting and Contact Lines of Micrometer-Sized Ellipsoids. *Phys. Rev. Lett.* **2006**, *97*, 018304.
(63) Park, B. J.; Furst, E. M. Attractive Interactions Between Colloids at the Oil-Water Interface. *Soft Matter* **2011**, *7*, 7676−7682.
(64) Zeng, C.; Brau, F.; Davidovitch, B.; Dinsmore, A. D. Capillary Interactions Among Spherical Particles at Curved Liquid Interfaces. *Soft Matter* **2012**, *8*, 8582−8594.
(65) Bigioni, T. P.; Lin, X.-M.; Nguyen, T. T.; Corwin, E. I.; Witten, T. A.; Jaeger, H. M. Kinetically Driven Self Assembly of Highly Ordered Nanoparticle Monolayers. *Nat. Mater.* **2006**, *5*, 265−270.
(66) Boley, J. W.; Hyun, S. H.; White, E. L.; Thompson, D. H.; Kramer, R. K. Hybrid Self-Assembly During Evaporation Enables Drop-on-Demand Thin Film Devices. *ACS Appl. Mater. Interfaces* **2016**, *8*, 34171−34178.
(67) Anyfantakis, M.; Geng, Z.; Morel, M.; Rudiuk, S.; Baigl, D. Modulation of the Coffee-Ring Effect in Particle/Surfactant Mixtures: The Importance of Particle-Interface Interactions. *Langmuir* **2015**, *31*, 4113−4120.
(68) Zhang, H.; Wang, W.; Hagen, N.; Kuzmenko, I.; Akinc, M.; Travesset, A.; Mallapragada, S.; Vaknin, D. Self-Assembly of DNA Functionalized Gold Nanoparticles at the Liquid-Vapor Interface. *Adv. Mater. Interfaces* **2016**, *3*, 1600180.
(69) Zhang, H.; Nayak, S.; Wang, W.; Mallapragada, S.; Vaknin, D. Interfacial Self-Assembly of Polyelectrolyte-Capped Gold Nanoparticles. *Langmuir* **2017**, *33*, 12227−12234.
(70) Anyfantakis, M.; Vialetto, J.; Best, A.; Auernhammer, G. K.; Butt, H.-J.; Binks, B. P.; Baigl, D. Adsorption and Crystallization of Particles at the Air−Water Interface Induced by Minute Amounts of Surfactant. *Langmuir* **2018**, *34*, 15526−15536.
(71) Li, Y.; Yang, Q.; Li, M.; Song, Y. Rate-Dependent Interface Capture Beyond the Coffee-Ring Effect. *Sci. Rep.* **2016**, *6*, 24628.
(72) Kim, D. O.; Pack, M.; Hu, H.; Kim, H.; Sun, Y. Deposition of Colloidal Drops Containing Ellipsoidal Particles: Competition Between Capillary and Hydrodynamic Forces. *Langmuir* **2016**, *32*, 11899−11906.
(73) Al-Milaji, K. N.; Secondo, R. R.; Ng, N. T.; Kinsey, N.; Zhao, H. Interfacial Self-Assembly of Colloidal Nanoparticles in Dual-Droplet Inkjet Printing. *Adv. Mater. Interfaces* **2018**, *5*, 1701561.
(74) Al-Milaji, K. N.; Radhakrishnan, V.; Kamerkar, P.; Zhao, H. pH-Modulated Self-Assembly of Colloidal Nanoparticles in a Dual-Droplet Inkjet Printing Process. *J. Colloid Interface Sci.* **2018**, *529*, 234−242.
(75) Ghafouri, A.; Zhao, M.; Singler, T. J.; Yong, X.; Chiarot, P. R. Interfacial Targeting of Sessile Droplets Using Electrospray. *Langmuir* **2018**, *34*, 7445−7454.
(76) Karapetsas, G.; Sahu, K. C.; Matar, O. K. Evaporation of Sessile Droplets Laden with Particles and Insoluble Surfactants. *Langmuir* **2016**, *32*, 6871−6881.
(77) Barmi, M. R.; Meinhart, C. D. Convective Flows in Evaporating Sessile Droplets. *J. Phys. Chem. B* **2014**, *118*, 2414−2421.
(78) Crivoi, A.; Duan, F. Three-Dimensional Monte Carlo Model of the Coffee-Ring Effect in Evaporating Colloidal Droplets. *Sci. Rep.* **2015**, *4*, 4310.
(79) Larson, R. G. Transport and Deposition Patterns in Drying Sessile Droplets. *AIChE J.* **2014**, *60*, 1538−1571.
(80) Bhardwaj, R.; Fang, X.; Attinger, D. Pattern Formation During the Evaporation of a Colloidal Nanoliter Drop: A Numerical and Experimental Study. *New J. Phys.* **2009**, *11*, 075020.
(81) Jafari Kang, S.; Vandadi, V.; Felske, J. D.; Masoud, H. Alternative Mechanism for Coffee-Ring Deposition Based on Active Role of Free Surface. *Phys. Rev. E: Stat. Phys., Plasmas, Fluids, Relat. Interdiscip. Top.* **2016**, *94*, 063104.
(82) Nguyen, T. A. H.; Biggs, S. R.; Nguyen, A. V. Manipulating Colloidal Residue Deposit from Drying Droplets: Air/Liquid Interface Capture Competes with Coffee-Ring Effect. *Chem. Eng. Sci.* **2017**, *167*, 78−87.
(83) Zhao, M.; Yong, X. Modeling Evaporation and Particle Assembly in Colloidal Droplets. *Langmuir* **2017**, *33*, 5734−5744.
(84) Zhao, M.; Yong, X. Nanoparticle Motion on the Surface of Drying Droplets. *Phys. Rev. Fluids* **2018**, *3*, 034201.
(85) Xu, T.; Lam, M. L.; Chen, T. H. Discrete Element Model for Suppression of Coffee-Ring Effect. *Sci. Rep.* **2017**, *7*, 42817.
(86) Yong, X.; Qin, S.; Singler, T. J. Nanoparticle-Mediated Evaporation at Liquid−Vapor Interfaces. *Extrem. Mech. Lett.* **2016**, *7*, 90−103.
(87) Cheng, S.; Grest, G. S. Molecular Dynamics Simulations of Evaporation-Induced Nanoparticle Assembly. *J. Chem. Phys.* **2013**, *138*, 064701.

DOI: 10.1021/acs.jpcc.9b00797
J. Phys. Chem. C 2019, 123, 12029−12041